Hydroxyl radical formation in the gas phase oxidation of distonic 2-methylphenyl radical cations

Abstract
The reactions of distonic 4-(N,N,N-trimethylammonium)-2-methylphenyl and 5-(N,N,N-trimethylammonium)-2-methylphenyl radical cations (m/z 149) with O 2 are studied in the gas phase using ion-trap mass spectrometry. Photodissociation (PD) of halogenated precursors gives rise to the target distonic charge-tagged methylphenyl radical whereas collision-induced dissociation (CID) is found to produce unreactive radical ions. The PD generated distonic radicals, however, react rapidly with O2 to form [M + O2]•+ and [M + O2 - OH]•+ ions, detected at m/z 181 and m/z 164, respectively. Quantum chemical calculations using G3SX(MP3) and M06-2X theories are deployed to examine key decomposition pathways of the 5-(N,N,N-trimethylammonium)-2-methylphenylperoxyl radical and rationalise the observed product ions. The prevailing product mechanism involves a 1,5-H shift in the peroxyl radical forming a QOOH-type intermediate that subsequently eliminates •OH to yield charge-tagged 2-quinone methide. Our study suggests that the analogous process should occur for the neutral methylphenyl + O2 reaction, thus serving as a plausible source of •OH radicals in combustion environments.

Keywords
phase, methylphenyl, gas, formation, radical, cations, hydroxyl, 2, distonic, oxidation

Disciplines
Medicine and Health Sciences | Social and Behavioral Sciences

Publication Details
Prendergast, M., Cooper, P. A., Kirk, B. B., da Silva, G., Blanksby, S. J. and Trevitt, A. J. (2013). Hydroxyl radical formation in the gas phase oxidation of distonic 2-methylphenyl radical cations. Physical Chemistry Chemical Physics, 15 (47), 20577-20584.

Authors
Matthew Prendergast, Phillip A. Cooper, Benjamin B. Kirk, Gabriel da Silva, Stephen J. Blanksby, and Adam J. Trevitt

PCCP

RSC Publishing

PAPER

View Article Online
View Journal | View Issue

Cite this: *Phys. Chem. Chem. Phys.*, 2013, **15**, 20577

Hydroxyl radical formation in the gas phase oxidation of distonic 2-methylphenyl radical cations†

Matthew B. Prendergast,[a] Phillip A. Cooper,[a] Benjamin B. Kirk,[ab] Gabriel da Silva,[c] Stephen J. Blanksby[ab] and Adam J. Trevitt*[ab]

Received 1st September 2013,
Accepted 21st October 2013

DOI: 10.1039/c3cp53690d

www.rsc.org/pccp

The reactions of distonic 4-(*N,N,N*-trimethylammonium)-2-methylphenyl and 5-(*N,N,N*-trimethylammonium)-2-methylphenyl radical cations (*m/z* 149) with O_2 are studied in the gas phase using ion-trap mass spectrometry. Photodissociation (PD) of halogenated precursors gives rise to the target distonic charge-tagged methylphenyl radical whereas collision-induced dissociation (CID) is found to produce unreactive radical ions. The PD generated distonic radicals, however, react rapidly with O_2 to form $[M + O_2]^{\bullet+}$ and $[M + O_2 - OH]^{\bullet+}$ ions, detected at *m/z* 181 and *m/z* 164, respectively. Quantum chemical calculations using G3SX(MP3) and M06-2X theories are deployed to examine key decomposition pathways of the 5-(*N,N,N*-trimethylammonium)-2-methylphenylperoxyl radical and rationalise the observed product ions. The prevailing product mechanism involves a 1,5-H shift in the peroxyl radical forming a QOOH-type intermediate that subsequently eliminates $^{\bullet}OH$ to yield charge-tagged 2-quinone methide. Our study suggests that the analogous process should occur for the neutral methylphenyl + O_2 reaction, thus serving as a plausible source of $^{\bullet}OH$ radicals in combustion environments.

1. Introduction

The study of aryl-radical + O_2 reactions is fundamental to understanding combustion chemistry due to the prevalence of aromatic hydrocarbons in liquid transportation fuels. Considerable work has been performed on the phenyl radical ($C_6H_5^{\bullet}$) and its reactions with O_2.[1–10] Notably, phenyl oxidation does not follow the ROO → QOOH isomerisation route often encountered when rationalising hydrocarbon radical oxidation;[11] instead, more elaborate peroxyl radical isomerisation channels are accessed. For substituted phenyl radicals there remains significant uncertainty around the key mechanisms and dominant reaction products in their oxidation.

Toluene ($C_6H_5CH_3$) is utilised in transportation fuels at high levels because of its high energy density and research octane number[12,13] and is also an intermediate in schemes of polycyclic aromatic hydrocarbon (PAH) and soot formation.[14] The primary combustion intermediate associated with toluene is generally considered to be the benzyl radical ($C_6H_5CH_2^{\bullet}$), rather than methylphenyl radical isomers ($C_6H_4CH_3^{\bullet}$), due to the relatively large difference in C–H bond dissociation energies for methyl (*ca.* 90 kcal mol^{-1}) and ring (*ca.* 113 kcal mol^{-1}) hydrogens.[15] Despite the difference in bond dissociation energies, abstraction reactions by reactive free radicals are expected to provide significant yields of methylphenyl radicals; for instance at 1000 K the product branching ratio for methylphenyl and benzyl radicals by $^{\bullet}OH$ abstraction reactions is close to 1 : 3, increasing to 1 : 2 at 2000 K.[16] The toluene C–CH_3 bond scission, yielding the phenyl radical, is also significant during thermal decomposition: 20% at 1200 K, and 40% at 1500 K.[17] Likewise, decomposition of poly-methyl substituted benzenes, such as *ortho*-xylene, can produce methylphenyl radicals.[18,19] Isomerisation of the methylphenyl radical to benzyl radical is generally competitive under high-temperature combustion conditions, however lifetimes of methylphenyl species near autoignition temperatures (~1000 K) are such as to permit bimolecular reactions with O_2.[19,20] Despite their plausible contribution in combustion environments, the methylphenyl + O_2 reaction has received relatively little attention. One computational study has suggested that the 2-methylphenyl + O_2 reaction is substantially different from that of the unsubstituted phenyl radicals, in which formation of 2-quinone methide + $^{\bullet}OH$ is thought to compete (*via* a process shown in Scheme 1) with phenylperoxyl-type isomerisation.[18] Experimental investigation of the methylphenyl + O_2 system can further the current understanding of toluene oxidation. However, identification and characterisation of

[a] *School of Chemistry, University of Wollongong, Wollongong, NSW 2522, Australia. E-mail: adamt@uow.edu.au*
[b] *ARC Centre of Excellence for Free Radical Chemistry and Biotechnology, University of Wollongong, NSW 2522, Australia*
[c] *Department of Chemical and Biomolecular Engineering, The University of Melbourne, VIC 3010, Australia*

† Electronic supplementary information (ESI) available. See DOI: 10.1039/c3cp53690d

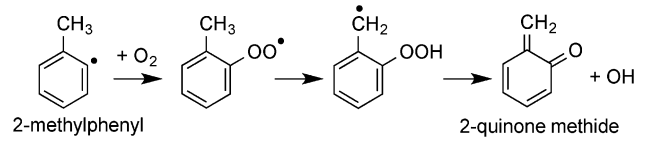

Scheme 1

reaction intermediates and products remain a challenge. Charge-tagged derivatives of the methylphenyl radicals, *i.e.* the addition of a substituent with a formal charge, can be employed *via* mass spectrometry to qualitatively assess dominant reaction processes. Here, we provide the first experimental evaluation of 2-methylphenyl + O_2 reaction using the distonic radical ion approach.

Distonic ions are radical ions characterised by the spatial and electronic separation of the radical and charge site.[21–23] Though the intrinsic reactivity of the radical may be perturbed to some degree by the presence of a near-by charge[24] studies on distonic radical ions undertaken using mass spectrometry nonetheless provide useful information on the reactions of their neutral counterparts.[24–27] A distonic radical ion approach has previously been employed to probe the fate of peroxyl radical intermediates; including, pyridinium-2-ethylperoxyl radical cation,[28,29] *N*-methylpyridinium-4-peroxyl[27,30] and 4-(*N*,*N*,*N*-trimethylammonium)phenylperoxyl radical cation,[27,31,32] in addition to 4-(*N*,*N*,*N*-trimethylammoniummethyl)phenylperoxyl, 3-(*N*,*N*,*N*-trimethylammonium)phenylperoxyl, and 4-ammoniumphenylperoxyl radical cations.[32] In each case, these distonic studies provided insight into the reactivity of the neutral radical analogue.

In this report we investigate the gas-phase synthesis and oxidation of distonic 2-methylphenyl radical cations. Radicals generated in a linear ion-trap mass spectrometer by both photodissociation (PD) and collision-induced dissociation (CID) of suitable halogenated precursors are compared and the dehalogenated radical cations are characterised by reactions with O_2. CID generated radical cations are found to exhibit low reactivity with O_2 on the timescale of the experiment (up to 10 s) suggesting that CID results in concomitant isomerisation, forming an unreactive radical ion isomer. In contrast, the PD generated radical cations readily react with O_2 to form the peroxyl radical that is followed by a H-atom shift and •OH elimination, consistent with the formation of charge-tagged 2-quinone methide product. This reaction scheme is supported by quantum chemical calculations.

2. Experimental

2.1 Materials

4-Bromo-3-methylaniline (97%), 3-bromo-4-methylaniline (98%), and methyl iodide (99.5%) were purchased from Sigma Aldrich (Milwaukee, USA). 3-Iodo-4-methylaniline (98%) was purchased from Alfa Aesar (Ward Hill, USA). 4-(Dimethylamino)benzyl alcohol was purchased from TCI Chemicals (Tokyo, Japan). Acetonitrile, ethyl acetate, methanol (HPLC grade), petroleum ether and potassium carbonate (anhydrous) were purchased from Ajax (Sydney, Australia). Industrial grade O_2 was obtained from BOC gases (Sydney, Australia). All commercial compounds were used without additional purification.

4-Bromo-*N*,*N*,*N*,3-tetramethylbenzenaminium (**4Br3Me**), 3-bromo-*N*,*N*,*N*,4-tetramethylbenzenaminium (**3Br4Me**) and 3-iodo-*N*,*N*,*N*,4-tetramethylbenzenaminium (**3I4Me**) iodide salts were synthesised by *N*-methylation of the corresponding primary amines listed above using a method previously described[31] with modifications detailed in Section S1 of the ESI.† 4-Iodomethyl-*N*,*N*,*N*-trimethylbenzenaminium (**4IMe**) iodide was synthesised from 4-(dimethylamino)benzyl alcohol by *N*-methylation[31] followed by iodo-dehydroxylation.[33] Synthesised compounds were characterised by ^{1}H NMR, data provided in Section S2 (ESI†).

2.2 Mass spectrometry

Experiments were performed on a modified Thermo Fisher Scientific LTQ linear quadrupole ion-trap mass spectrometer (San Jose, USA)[34] fitted with an IonMax electrospray ionisation source operated in positive ion mode (+ESI) and controlled by Xcalibur 2.0 software. Ions were generated by infusing 5–15 μM methanolic solutions of 4-bromo-*N*,*N*,*N*,3-tetramethylbenzenaminium (**4Br3Me**), 3-bromo-*N*,*N*,*N*,4-tetramethylbenzenaminium (**3Br4Me**), 3-iodo-*N*,*N*,*N*,4-tetramethylbenzenaminium (**3I4Me**), and 4-iodomethyl-*N*,*N*,*N*-trimethylbenzenaminium (**4IMe**) iodide salts into the electrospray ion source at 5 μL min^{-1}. Typical instrumental settings were: spray voltage (4.5 kV), capillary temperature (200 °C), sheath gas flow at 5 (arbitrary units), sweep and auxiliary gas flow at 10 (arbitrary units). Ions were mass-selected using an isolation window of 5–6 Th for **4Br3Me** and **3Br4Me**, and 1–2 Th for **3I4Me** and **4IMe** with a *q*-parameter of 0.250. Mass spectra presented herein are the average of at least 50 scans. In CID experiments, the normalised collision energy applied was typically 20–30 (arbitrary units) with an activation time of 30 ms set within the control software.

2.2.1 Photodissociation (PD). The modifications to the ion-trap mass spectrometer allowing optical access to trapped ions are similar to those previously reported[35,36] and are described in detail elsewhere.[37,38] Briefly, a 10 mm aperture was milled into the removable backplate of the vacuum chamber. A 2.75 inch quartz viewport was mounted over the aperture with a CF flange. At the beginning of a MS^n ion activation step, the mass spectrometer transmits a TTL-signal to a digital delay generator that subsequently triggers a Nd:YAG laser (operating on the 4th harmonic, λ = 266 nm) such that only a single laser pulse is generated per duty cycle. The λ = 266 nm laser pulse (*ca.* 30 mJ cm^{-2}) is transmitted through the quartz window and 2 mm orifice centred on the back lens of the ion-trap assembly allowing for PD of isolated ionic species.

2.2.2 Ion–molecule reactions. O_2 is present in background concentrations due to the use of an atmospheric pressure ionisation source. Typically, N_2 is used as the nebulising gas within the ionisation source, however, to increase the background O_2 concentration, O_2 can be used instead. The O_2 concentration (molecule cm^{-3}) within the ion trap region was derived by following the 4-(*N*,*N*,*N*-trimethylammonium)phenyl radical + O_2 reaction kinetics, which has a known second-order rate coefficient (k_{2nd}) of 2.8 × 10^{-11} cm^3 molecule^{-1} s^{-1}.[31]

The O_2 concentration within the ion trap was measured at 2.2×10^9 molecule cm^{-3} for background O_2 with the standard nitrogen nebuliser gas, and 8.6×10^9 molecule cm^{-3} with O_2 used as the nebuliser gas.

The stoichiometric excess of O_2, by many orders of magnitude, established pseudo-first order kinetic behaviour with reactive ions.[34,39] The temperature within the ion trap was previously measured at 307 ± 1 K (ref. 39 and 40) and is used as the effective temperature for ion–molecule reactions herein. This is consistent with recent measurements by Donald *et al.* of 318 ± 23 K.[41] Reaction times of 0.030–10 s were achieved by setting the activation time parameter with the control software while the normalised collision energy was maintained at 0 (arbitrary units).[42] Measured pseudo-first order (k') and second-order (k_{2nd}) rate coefficients were extracted from the slope of a semi-logarithmic plot of normalised abundance against reaction time.

Statistical errors in rate measurements were typically $2\sigma < 5\%$, where σ is the standard deviation obtained from the least-squares fit to the pseudo-first order decay. Systematic uncertainty in the ion-trap pressure and O_2 concentration, and the formation of neutrals or ions with a *m/z* less than the low mass cut-off (*ca.* 50 Th) result in a upper limit of 50% uncertainty in second-order rate coefficients (k_{2nd}). Reported reaction efficiencies are calculated from the second-order rate coefficient as a percentage of the reactants' collision frequency derived from average dipole orientation (ADO) theory.[43]

2.3 Quantum chemical calculations

Electronic structure calculations were performed using both the M06-2X/6-311++G(d,p) density functional theory[44] and G3SX(MP3) composite method,[45] in the Gaussian 09 program.[46] All stationary points were characterised as either minima (no imaginary frequencies) or transition states (one imaginary frequency). All reported energies are at 0 K and include zero-point energy corrections. The selected theoretical methods are capable of reproducing well-defined test set barrier heights to within 1.5 kcal mol^{-1}, on average.[45,47]

3. Results and discussion

3.1 Synthesis of distonic 2-methylphenyl radical cations

Two synthetic routes for the production of radical cations within the linear ion-trap mass spectrometer were compared: laser photodissociation (PD) and collision-induced dissociation (CID). Methanolic solutions of the precursor iodide salts were infused *via* positive electrospray ionisation (+ESI) to yield the M^+ ions at *m/z* 228 and 230 for the brominated (**4Br3Me** and **3Br4Me**), and *m/z* 276 for the iodinated (**3I4Me** and **4IMe**) precursor ions, as listed in Table 1.

Isolation and subsequent PD of the M^+ ions listed in Table 1 resulted in *m/z* 149 product ions consistent with the loss of the halogen atom (ESI,† Fig. S1). PD of the brominated precursors **4Br3Me** and **3Br4Me** resulted also in $[M - Br - 15]^{\bullet+}$ signal at *m/z* 134 and $[M - CH_3]^+$ signal at *m/z* 213 and 215. In the case of PD of the iodinated precursors **3I4Me** and **4IMe**, *m/z* 134 is also apparent and likely corresponds to $[M - I - CH_3]^{\bullet+}$.

Table 1 Distonic radical precursor ions $[M]^+$ introduced by +ESI of methanolic solutions of the corresponding salt

Precursor ions $[M]^+$	Structure	Abbreviation
4-Bromo-*N,N,N*,3-tetramethylbenzenaminium cation (*m/z* 228 and 230)	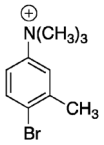	**4Br3Me**
3-Bromo-*N,N,N*,4-tetramethylbenzenaminium cation (*m/z* 228 and 230)	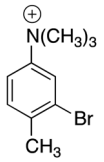	**3Br4Me**
3-Iodo-*N,N,N*,4-tetramethylbenzenaminium cation (*m/z* 276)	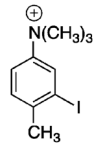	**3I4Me**
4-(Iodomethyl)-*N,N,N*-trimethylbenzenaminium cation (*m/z* 276)	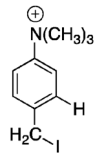	**4IMe**

The dominant product observed after CID of **4Br3Me**, **3Br4Me**, and **3I4Me** was the $[M - 15]^{\bullet+}$ ion at *m/z* 213 and 215 for the brominated species (both Br isotopes), and *m/z* 261 for **3I4Me**. These odd-electron processes are consistent with $^{\bullet}CH_3$ loss from the trimethylammonium charge tag of the respective M^+ ions. Minor ion signal at *m/z* 149 is assigned to ejection of the halogen. In contrast, CID of **4IMe** resulted predominately in the *m/z* 149 and 134 ions, assigned as loss of $I^{\bullet}$ followed by elimination of a methyl radical from the charge tag, respectively.

Activation of **4Br3Me**, **3Br4Me**, **3I4Me**, and **4IMe** ions by both PD and CID resulted in formation of *m/z* 149 ions with varying efficiencies. PD of the **4Br3Me**, **3Br4Me**, and **3I4Me** halogenated precursors resulted in significantly higher abundances of the putative distonic radical ion (*ca.* 25–45%) than CID (*ca.* <2%). In contrast, CID of the **4IMe** ion resulted in a notably higher abundance of the *m/z* 149 ion (*ca.* 90%) than that observed for the PD route (*ca.* 10%). In each case, the *m/z* 149 ion population was isolable and probed by reactions with O_2.

3.2 Charge-tagged 2-methylphenyl + O_2

The *m/z* 149 ions generated by PD and CID of **4Br3Me**, **3Br4Me**, **3I4Me** and **4IMe** were isolated and allowed to react with background O_2 over time periods of 0.030–10 s. Mass spectra measured with a reaction time of 2 s are provided in Fig. 1. Second-order rate coefficients (k_{2nd}) were derived and are discussed below in Section 3.2.1. Isolation of *m/z* 149 ions, generated by PD of **4Br3Me**, **3Br4Me**, and **3I4Me**, in the presence of background O_2 resulted in a small $[M + 32]^{\bullet+}$ product ion signal at *m/z* 181, consistent with the formation of a peroxyl radical.

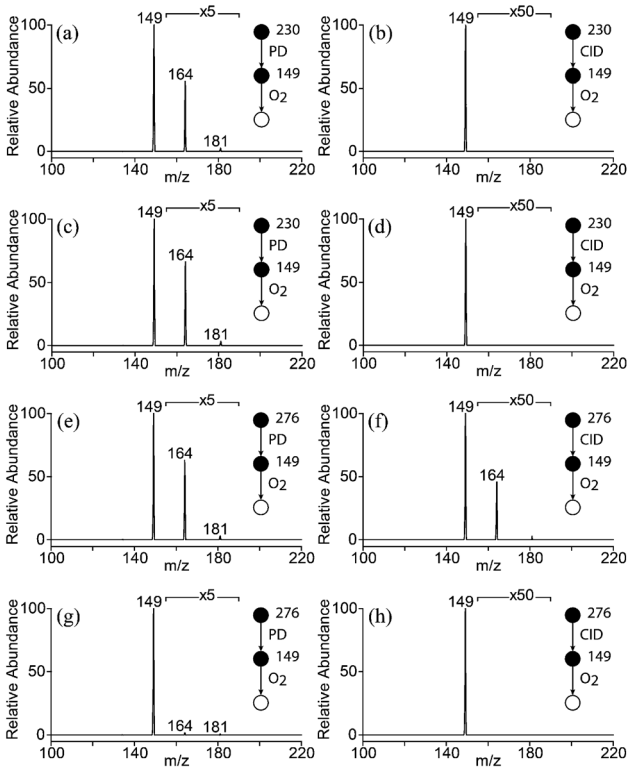

Fig. 1 PD (left panel) and CID (right panel) mass spectra of **4Br3Me** (a and b), **3Br4Me** (c and d), **3I4Me** (e and f) and **4IMe** (g and h) isolated for a period of 2 s in the presence of background O_2. Trace ions at *m/z* 164 and 181 observed in (g) are likely the result of contamination by isomeric distonic radical cations.

The dominant product observed was the $[M + 15]^{\bullet+}$ ion at *m/z* 164 rationalised by O_2 addition and subsequent $^{\bullet}OH$ elimination, as depicted in Scheme 2. This is consistent with the $^{\bullet}OH$ elimination mechanism proposed in the theoretical study of the analogous neutral 2-methylphenyl radical + O_2 reaction by da Silva *et al.*[18] (Scheme 1). CID of *m/z* 164 ions (ESI,† Fig. S2) gives rise to *m/z* 149, presumably the result of CH_3 (15 Da) loss from the trimethylammonium charge tag. There is also a product ion consistent with CO (28 Da) loss at *m/z* 136, and another at *m/z* 121 consistent with both loss of CH_3 and CO. The primary fragmentation pathway for the neutral 2-quinone methide is loss of CO.[48,49] A more detailed mechanism and energy schematic, including the formation of *m/z* 164, will be outlined below. The reactions of *m/z* 149 ions with O_2, after PD of **4IMe**, yielded only traces of oxidation products likely the result of contamination by isomeric distonic radical cations as the majority of the *m/z* 149 species is likely to be the resonance stabilised benzyl radical.

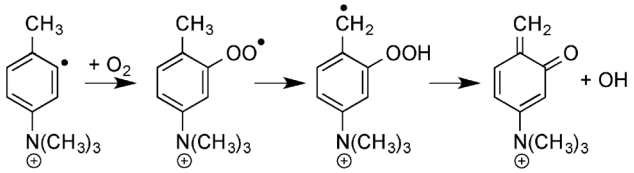

Scheme 2

Prolonged isolation (up to 10 s) of *m/z* 149 ions generated by CID of **4Br3Me**, **3Br4Me**, and **4IMe** under the same experimental conditions [Fig. 1(b), (d) and (h)] did not result in observable $[M + O_2]^{\bullet+}$ or $[M + O_2 - OH]^{\bullet+}$ product ions, while isolation of *m/z* 149 ions from CID of **3I4Me** resulted in only low intensity signals at corresponding *m/z* ratios [Fig. 1(e) with ×5 magnification compared to Fig. 1(f) with ×50]. The low abundance, or even absence, of the respective $[M + O_2]^{\bullet+}$ and $[M + O_2 - OH]^{\bullet+}$ ions, when compared with analogous PD experiments, suggests that the *m/z* 149 ions resulting from CID of **4Br3Me** and **3Br4Me** are less reactive isomeric species born from CID-induced rearrangement. The isomerisation of phenyl-type radical cations upon CID of halogenated precursors has been previously noted.[50] Herein, PD was used for all subsequent experiments.

3.2.1 Reaction kinetics. The reactions of PD generated *m/z* 149 ions with O_2 were further characterised by second-order rate coefficients (k_{2nd}, cm^3 $molecule^{-1}$ s^{-1}) and reaction efficiencies (Φ), reported in Table 2, derived from measured pseudo-first order rate coefficients at background O_2 ($[O_2] = 2.23 \times 10^9$ molecule cm^{-3}) and increased O_2 concentrations ($[O_2] = 8.53 \times 10^9$ molecule cm^{-3}). The O_2 collision frequency calculated with average dipole orientation (ADO) theory[43] is 5.7×10^{-10} cm^3 $molecule^{-1}$ s^{-1} for all species of *m/z* 149. Pseudo-first order kinetic behaviour, as shown by a linear semi-logarithmic plot (Fig. 2), is observed for *m/z* 149 ions generated by PD of **4Br3Me**, **3Br4Me** and **3I4Me**, implying that each of these radical ion populations consist of only a single species.[50,51] The general agreement between k_{2nd} values for radical ions generated by PD

Table 2 Second-order rate coefficients (k_{2nd}, cm^3 $molecule^{-1}$ s^{-1}) and reaction efficiencies (Φ) for reactions of PD generated distonic radicals with O_2 (molecule cm^{-3}). Estimated upper limit of 50% uncertainty in second-order rate coefficients. O_2 collision frequency from average dipole orientation (ADO) theory[43] is 5.7×10^{-10} cm^3 $molecule^{-1}$ s^{-1} for all species of *m/z* 149

Precursor ions	Distonic radicals	$[O_2]$ (molecule cm^{-3})	k_{2nd} (cm^3 $molecule^{-1}$ s^{-1})	Φ (%)
4Br3Me	4-(*N*,*N*,*N*-Trimethylammonium)-2-methylphenyl	2.23×10^9	2.4×10^{-11}	4.1
		8.53×10^9	2.1×10^{-11}	3.7
3Br4Me	5-(*N*,*N*,*N*-Trimethylammonium)-2-methylphenyl	2.23×10^9	2.9×10^{-11}	5.1
		8.53×10^9	2.6×10^{-11}	4.5
3I4Me	5-(*N*,*N*,*N*-Trimethylammonium)-2-methylphenyl	2.23×10^9	2.8×10^{-11}	5.0
		8.53×10^9	2.6×10^{-11}	4.6
4IMe	4-(*N*,*N*,*N*-Trimethylammonium)-benzyl	2.23×10^9	—	—
		8.53×10^9	—	—

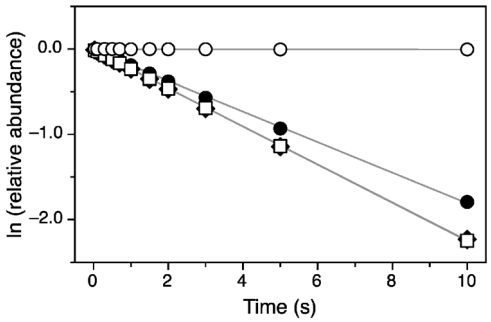

Fig. 2 Semi-logarithmic plot for depletion of *m/z* 149 ions generated by PD of **4Br3Me** (closed circles), **3Br4Me** (diamonds), **3I4Me** (squares) and **4IMe** (open circles) precursors ions, in reactions with O_2 ($[O_2] = 8.53 \times 10^9$ molecule cm^{-3}). Second-order rate coefficients provided in Table 2.

of **3Br4Me** and **3I4Me** suggests the identity of the radical formed by λ = 266 nm photolysis is unaffected by the halogen substituent on the radical precursor. Rate coefficients for *m/z* 149 from PD of **3Br4Me** and **4Br3Me** reveal a slight, but reproducible, difference in reaction rate where the radical is at the 3- over the 4-position relative to the charge-tag, *i.e.*, $k_{3Br4Me} > k_{4Br3Me}$. This effect could be due to small differences in the electrophilicity of the two positive distonic radical ions[24,52] but overall the reaction efficiencies are very similar to each other and to previous measurements for phenyl-type radicals. For example, the measured reaction efficiencies in Table 2 are similar to those reported by Kirk *et al.*[31] for positively charge-tagged distonic phenyl radicals (about 5%), suggesting, intriguingly, that the methyl substituent, although presenting a new reaction pathway, does not drastically alter the overall reaction efficiency. More discussion on the reaction pathway is provided below.

The *m/z* 149 species generated by PD of **4IMe**, expected to provide a benzylic radical ion for comparison, was unreactive on the timescale of these experiments (0.030–10 s). The addition of O_2 to the neutral benzyl radical is reported to produce a benzylperoxyl radical with a reaction exothermicity of 22 kcal mol^{-1}; however, reformation of benzyl + O_2 reactants dominates at low temperatures.[53] In the analogous charge-tagged benzyl radical + O_2 reaction, it is expected that upon O_2 addition the vibrationally excited charge-tagged benzylperoxyl radical will dissociate to regenerate the charge-tagged benzyl + O_2 before being collisionally deactivated in the ion trap or undergoing further unimolecular reaction.

3.2.2 Reaction mechanism. Fig. 3 depicts a potential energy diagram for the addition of O_2 to the 5-(*N,N,N*-trimethylammonium)-2-methylphenyl radical cation (generated by PD of **3Br4Me** or **3I4Me**). This scheme essentially reproduces the reaction mechanism identified in the analogous neutral system.[18] Energies were calculated using the M06-2X/6-311++G(d,p) (black) and G3SX(MP3) (blue) methods, reported in kcal mol^{-1} relative to the peroxyl radical intermediate. The ensuing discussion will refer to the G3SX(MP3) energies.

The addition of O_2 to the charge-tagged 2-methylphenyl radical (**I**) proceeds without a barrier and results in a charge-tagged methylphenylperoxyl species (**II**) with 46.4 kcal mol^{-1} activation. Fig. 3 depicts four low-energy unimolecular reaction pathways available to the charge-tagged 2-methylphenylperoxyl radical. First, the reverse reaction reforms the distonic 2-methylphenyl radical + O_2 (**I**); second, formation of a phenoxyl radical + $O(^3P)$ (**III**); third, isomerisation to methyloxepinoxyl species (**V** and **VI**); and fourth, the generation of charge-tagged 2-quinone methide + $^{\bullet}OH$ (**VIII**). In the context of

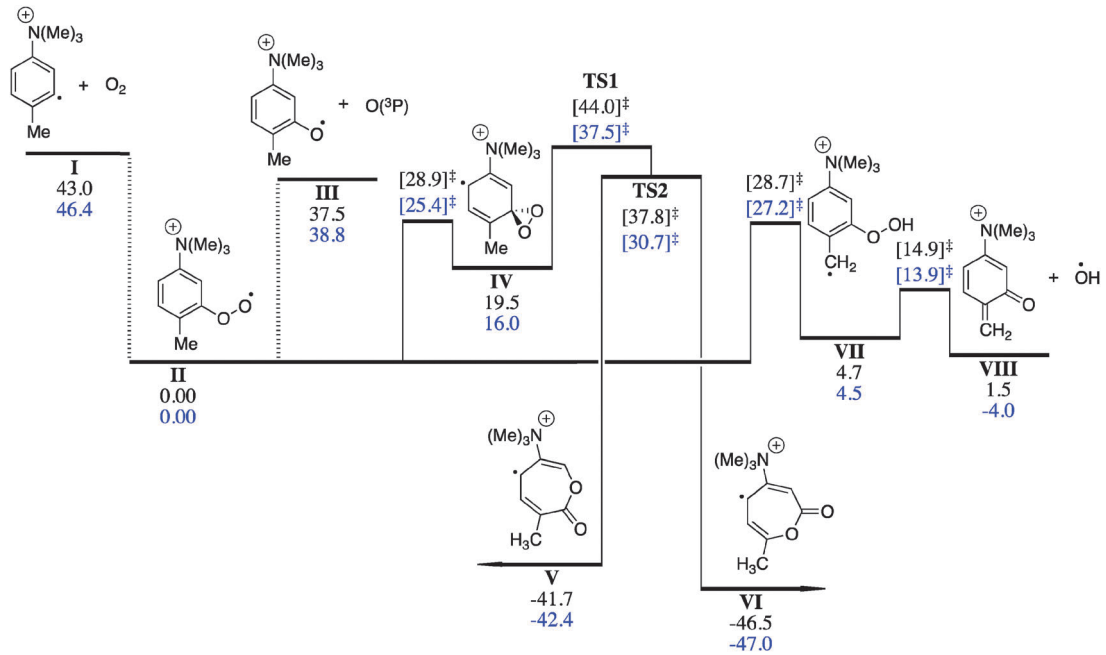

Fig. 3 Potential energy diagram depicting key intermediates for *N,N,N*-trimethylammonium charged-tagged 2-methylphenyl radical cation + O_2. Energies were calculated at the M06-2X/6-311++G(d,p) (black) and G3SX(MP3) (blue) levels, reported in kcal mol^{-1} relative to the initial intermediate.

forming new product species, the latter three pathways will be discussed further below.

Formation of 5-(*N,N,N*-trimethylammonium)-2-methylphenoxyl + $O(^3P)$ (**III**) occurs *via* cleavage of the peroxyl RO–O bond. Delocalisation of the unpaired electron is evidenced by a predicted contraction of the C–O bond from 1.392 Å in the peroxyl to 1.235 Å in the phenoxyl, closer to that expected for a CO double bond. The barrier for this process is calculated at 38.8 kcal mol^{-1} compared with 46.4 kcal mol^{-1} for the reactants. The $O(^3P)$ loss mechanism would result in a *m/z* 165 ion corresponding to the 16 Da mass loss. Subsequent CO loss from this phenoxyl radical[10] would result in an $[M + O_2 - O - CO]^{\bullet+}$ ion at *m/z* 137. Neither O atom nor CO loss product ions were observed within the detection limits of the experiment pointing to a lack of competitiveness for this pathway. Other accessible pathways outcompete the $O(^3P)$ loss channel as shown by the dominance of alternate product channels in Fig. 1.

The third pathway from **II** proceeds by *ipso* addition of the peroxyl radical oxygen to the aromatic ring (**TS II → IV**, 25.4 kcal mol^{-1}) resulting in the dioxiranyl intermediate (**IV**). The sequential transition states, **TS1** (37.5 kcal mol^{-1}) and **TS2** (30.7 kcal mol^{-1}), succeeding the dioxiranyl intermediate, represent a bifurcation[54] of the potential energy surface. Following the intrinsic reaction coordinate (IRC) from **TS1**, reactive species encounter a valley-ridge inflection (VRI) near which the single reaction pathway becomes two. Past the VRI, along the developing ridge, the second transition state (**TS2**) is located, which connects the charge-tagged 3-methyloxepinoxyl (**V**) and 7-methyloxepinoxyl (**VI**) species (confirmed by calculation of the IRC for **TS2**). Ring-opening of the dioxiranyl moiety (**TS1**), *i.e.*, cleavage of the dioxiranyl O–O bond, has a barrier that is 8.9 kcal mol^{-1} less than the chemical activation of the system. At these temperatures (*ca.* 307 K), we do not expect any significant reaction flux through **TS1** due to its high energy (37.5 kcal mol^{-1}), thus these pathways were not extended beyond the methyloxepinoxy radicals (**V** and **VI**). Guided by Kirk *et al.*,[31] it is likely the end-product species could comprise five-membered ring products, such as a charge-tagged methyl-substituted cyclopentadienone species but no such channels were detected in our charge-tagged experiments. This implicates the presence of lower-energy reaction pathways not available to the charge-tagged phenylperoxyl radical systems investigated by Kirk *et al.*

The final pathway considered here leads to charge-tagged 2-quinone methide *via* H-migration followed by $^{\bullet}OH$ elimination. The 1,5-H shift *via* **TS II → VII** proceeds with a 27.2 kcal mol^{-1} barrier (19.1 kcal mol^{-1} below the reactants' energy) and results in a hydroperoxybenzyl radical species (**VII**), reminiscent of a QOOH combustion intermediate. The formation of this radical is facilitated by close proximity of the labile benzylic methyl hydrogen to the peroxyl group.[18] The forward reaction barrier of 9.4 kcal mol^{-1} for **TS VII → VIII** is considerably less than that for the reverse reaction (22.7 kcal mol^{-1}). Thus, H atom migration and $^{\bullet}OH$ elimination is energetically competitive and results in the formation of charge-tagged 2-quinone methide (**VIII**), consistent with the $[M + O_2 - OH]^{\bullet+}$ ion detected at *m/z* 164, shown in Fig. 1 (left panel).

The G3SX(MP3) and M06-2X methods both predict, based purely on reaction barriers, the dominance of the charge-tagged 2-quinone methide + $^{\bullet}OH$ product channel and the numbers are generally in good agreement. The greatest deviations were observed for **TS1** and **TS2**, with a difference of 6.5 and 7.1 kcal mol^{-1} (Table S2, ESI†). These are perhaps more peculiar stationary points and could warrant future investigation. Nevertheless, both methods are in agreement that the **TS1** barrier is likely to be prohibitively high. The scheme depicted in Fig. 3 supports the notion that H-atom migration followed by $^{\bullet}OH$ elimination is the dominant product channel. This is in agreement with experimental data that shows charge-tagged 2-methylphenyl radicals react with O_2 to eliminate $^{\bullet}OH$, forming the $[M + 15]^{\bullet+}$ ion detected at *m/z* 164 consistent with the charge-tagged 2-quinone methide.

4. Conclusions

The reaction of two distonic radical ions [4-(*N,N,N*-trimethylammonium)-2-methylphenyl and 5-(*N,N,N*-trimethylammonium)-2-methylphenyl radicals] with O_2 were successfully used to explore the 2-methylphenyl + O_2 reaction. Subjecting the halogenated precursors **4Br3Me**, **3Br4Me** and **3I4Me** to PD resulted in exclusive formation of the distonic radical ion targets, while CID of the same precursors led to complications due to isomerisation to an unreactive isomeric species. The distonic 2-methylphenyl radical + O_2 reaction gave rise to $[M + O_2]^{\bullet+}$ and $[M + O_2 - OH]^{\bullet+}$ ions from O_2 addition followed by $^{\bullet}OH$ elimination as the dominant oxidation product. Second-order rate coefficients for these reactions were measured between 2.1–2.9 × 10^{-11} cm^3 $molecule^{-1}$ s^{-1} representing reaction efficiencies of *ca.* 5%. Quantum chemical calculations are in accord with our experimental observations, where H migration and $^{\bullet}OH$ elimination, *via* the QOOH intermediate, is the minimum energy pathway and should thus dominate product formation. The proposed generation of the charge-tagged 2-quinone methide suggests similar processes may occur in the neutral system and therefore serve as a $^{\bullet}OH$ radical source for further radical chemistry in reactive environments.

Acknowledgements

The authors are grateful for the financial support of the Australian Research Council through the Discovery program (SJB: DP0986738; AJT and GdS: DP 130100862; GdS: DP110103889) and Centre of Excellence For Free Radical Chemistry and Biotechnology (CE0561607). The authors also acknowledge the generous allocation of computing resources by the NCI National Facility (Canberra, Australia) under Merit Allocation Scheme.

References

1 C. Barckholtz, M. J. Fadden and C. M. Hadad, Computational Study of the Mechanisms for the Reaction of $O_2(3\Sigma_g)$ with Aromatic Radicals, *J. Phys. Chem. A*, 1999, **103**, 8108–8117.
2 B. K. Carpenter, Computational Prediction of New Mechanisms for the Reactions of Vinyl and Phenyl Radicals with Molecular Oxygen, *J. Am. Chem. Soc.*, 1993, **115**, 9806–9807.

3 B. K. Carpenter, Ring Opening of Dioxiranylmethyl Radical: A Caution on the Use of G2-Type Ab Initio MO Methods for Mechanistic Analysis, *J. Phys. Chem. A*, 2001, **105**, 4585–4588.
4 G. da Silva and J. W. Bozzelli, Variational Analysis of the Phenyl + O_2 and Phenoxy + O Reactions, *J. Phys. Chem. A*, 2008, **112**, 3566–3575.
5 M. J. Fadden, C. Barckholtz and C. M. Hadad, Computational Study of the Unimolecular Decomposition Pathways of Phenylperoxy Radical, *J. Phys. Chem. A*, 2000, **104**, 3004–3011.
6 M. J. Fadden and C. M. Hadad, Unimolecular Decomposition of the 2-Oxepinoxy Radical: A Key Seven-Membered Ring Intermediate in the Thermal Oxidation of Benzene, *J. Phys. Chem. A*, 2000, **104**, 8121–8130.
7 R. P. Lindstedt and G. Skevis, Detailed Kinetic Modeling of Premixed Benzene Flames, *Combust. Flame*, 1994, **99**, 551–561.
8 A. M. Mebel and M. C. Lin, Ab Initio Molecular Orbital Calculations of $C_6H_5O_2$ Isomers, *J. Am. Chem. Soc.*, 1994, **116**, 9577–9584.
9 N. Sebbar, H. Bockhorn and J. Bozzelli, Thermodynamic Properties of the Species Resulting from the Phenyl Radical with O_2 Reaction System, *Int. J. Chem. Kinet.*, 2008, **40**, 583–604.
10 I. V. Tokmakov, G.-S. Kim, V. V. Kislov, A. M. Mebel and M. C. Lin, The Reaction of Phenyl Radical with Molecular Oxygen: A G2M Study of the Potential Energy Surface, *J. Phys. Chem. A*, 2005, **109**, 6114–6127.
11 J. Zádor, C. A. Taatjes and R. X. Fernandes, Kinetics of Elementary Reactions in Low-Temperature Autoignition Chemistry, *Prog. Energy Combust. Sci.*, 2011, **37**, 371–421.
12 J. F. Griffiths, P. A. Halford-Maw and D. J. Rose, Fundamental Features of Hydrocarbon Autoignition in a Rapid Compression Machine, *Combust. Flame*, 1993, **95**, 291–306.
13 G. da Silva and J. W. Bozzelli, On the Reactivity of Methylbenzenes, *Combust. Flame*, 2010, **157**, 2175–2183.
14 T. R. Melton, F. Inal and S. M. Senkan, The Effects of Equivalence Ratio on the Formation of Polycyclic Aromatic Hydrocarbons and Soot in Premixed Ethane Flames, *Combust. Flame*, 2000, **121**, 671–678.
15 S. J. Blanksby and G. B. Ellison, Bond Dissociation Energies of Organic Molecules, *Acc. Chem. Res.*, 2003, **36**, 255–263.
16 T. Seta, M. Nakajima and A. Miyoshi, High-Temperature Reactions of OH Radicals with Benzene and Toluene, *J. Phys. Chem. A*, 2006, **110**, 5081–5090.
17 M. A. Oehlschlaeger, D. F. Davidson and R. K. Hanson, Thermal Decomposition of Toluene: Overall Rate and Branching Ratio, *Proc. Combust. Inst.*, 2007, **31**, 211–219.
18 G. da Silva, C.-C. Chen and J. W. Bozzelli, Toluene Combustion: Reaction Paths, Thermochemical Properties, and Kinetic Analysis for the Methylphenyl Radical + O_2 Reaction, *J. Phys. Chem. A*, 2007, **111**, 8663–8676.
19 E. Dames and H. Wang, Isomerization Kinetics of Benzylic and Methylphenyl Type Radicals in Single-Ring Aromatics, *Proc. Combust. Inst.*, 2013, **34**, 307–314.
20 J. L. Emdee, K. Brezinsky and I. Glassman, Oxidation of o-Xylene, *Proc. Combust. Inst.*, 1990, **23**, 77–84.
21 W. J. Bouma, R. H. Nobes and L. Radom, Methylenoxonium Radical Cation ($CH_2OH_2^{\bullet+}$): A Surprisingly Stable Isomer of the Methanol Radical Cation, *J. Am. Chem. Soc.*, 1982, **104**, 2929–2930.
22 W. J. Bouma, J. K. MacLeod and L. Radom, Experimental Evidence for the Existence of a Stable Isomer of $CH_3OH^{+\bullet}$: The Methylenoxonium Radical Cation, $CH_2OH_2^{+\bullet}$, *J. Am. Chem. Soc.*, 1982, **104**, 2930–2931.
23 P. E. Williams, B. J. Jankiewicz, L. Yang and H. I. Kenttämaa, Properties and Reactivity of Gaseous Distonic Radical Ions with Aryl Radical Sites, *Chem. Rev.*, 2013, **113**, 6949–6985.
24 C. J. Petzold, E. D. Nelson, H. A. Lardin and H. I. Kenttämaa, Charge-Site Effects on the Radical Reactivity of Distonic Ions, *J. Phys. Chem. A*, 2002, **106**, 9767–9775.
25 K. M. Stirk, L. K. M. Kiminkinen and H. I. Kenttämaa, Ion-Molecule Reactions of Distonic Radical Cations, *Chem. Rev.*, 1992, **92**, 1649–1665.
26 B. B. Kirk, D. G. Harman and S. J. Blanksby, Direct Observation of the Gas Phase Reaction of the Cyclohexyl Radical with Dioxygen Using a Distonic Radical Ion Approach, *J. Phys. Chem. A*, 2010, **114**, 1446–1456.
27 C. H. Li, G. N. Khairallah, A. K. Y. Lam, R. A. J. O'Hair, B. B. Kirk, S. J. Blanksby, G. da Silva and U. Wille, Reaction of Aromatic Peroxyl Radicals with Alkynes: A Mass Spectrometric and Computational Study Using the Distonic Radical Ion Approach, *Chem.–Asian J.*, 2013, **8**, 450–464.
28 S. J. Yu, C. L. Holliman, D. L. Rempel and M. L. Gross, The β-Distonic Ion from the Reaction of Pyridine Radical Cation and Ethene: A Demonstration of High-Pressure Trapping in Fourier Transform Mass Spectrometry, *J. Am. Chem. Soc.*, 1993, **115**, 9676–9682.
29 A. E. P. M. Sorrilha, F. b. C. Gozzo, R. S. Pimpim and M. N. Eberlin, Multiple Stage Pentaquadrupole Mass Spectrometry for Generation and Characterization of Gas-Phase Ionic Species. The Case of the $PyC_2H_5^{\bullet+}$ Isomers, *J. Am. Soc. Mass Spectrom.*, 1996, **7**, 1126–1137.
30 A. K. Y. Lam, C. Li, G. Khairallah, B. B. Kirk, S. J. Blanksby, A. J. Trevitt, U. Wille, R. A. J. O'Hair and G. da Silva, Gas-Phase Reactions of Aryl Radicals with 2-Butyne: Experimental and Theoretical Investigation Employing the N-Methyl-Pyridinium-4-yl Radical Cation, *Phys. Chem. Chem. Phys.*, 2012, **14**, 2417–2426.
31 B. B. Kirk, D. G. Harman, H. I. Kenttämaa, A. J. Trevitt and S. J. Blanksby, Isolation and Characterization of Charge-Tagged Phenylperoxyl Radicals in the Gas Phase: Direct Evidence for Products and Pathways in Low Temperature Benzene Oxidation, *Phys. Chem. Chem. Phys.*, 2012, **14**, 16719–16730.
32 A. T. Maccarone, B. B. Kirk, C. S. Hansen, T. M. Griffiths, S. Olsen, A. J. Trevitt and S. J. Blanksby, Direct Observation of Photodissociation Products from Phenylperoxyl Radicals Isolated in the Gas Phase, *J. Am. Chem. Soc.*, 2013, **135**, 9010–9014.
33 S. M. Klein, C. Zhang and Y. L. Jiang, Simple Synthesis of Fresh Alkyl Iodides Using Alcohols and Hydriodic Acid, *Tetrahedron Lett.*, 2008, **49**, 2638–2641.
34 J. C. Schwartz, M. W. Senko and J. E. P. Syka, A Two-Dimensional Quadrupole Ion Trap Mass Spectrometer, *J. Am. Soc. Mass Spectrom.*, 2002, **13**, 659–669.

35 T. Ly and R. R. Julian, Residue-Specific Radical-Directed Dissociation of Whole Proteins in the Gas Phase, *J. Am. Chem. Soc.*, 2008, **130**, 351–358.
36 T.-Y. Kim, M. S. Thompson and J. P. Reilly, Peptide Photodissociation at 157 nm in a Linear Ion Trap Mass Spectrometer, *Rapid Commun. Mass Spectrom.*, 2005, **19**, 1657–1665.
37 T. Ly, B. B. Kirk, P. I. Hettiarachchi, B. L. J. Poad, A. J. Trevitt, G. da Silva and S. J. Blanksby, Reactions of Simple and Peptidic Alpha-Carboxylate Radical Anions with Dioxygen in the Gas Phase, *Phys. Chem. Chem. Phys.*, 2011, **13**, 16314–16323.
38 C. S. Hansen, B. B. Kirk, S. J. Blanksby, R. A. J. O'Hair and A. J. Trevitt, UV Photodissociation Action Spectroscopy of Haloanilinium Ions in a Linear Quadrupole Ion Trap Mass Spectrometer, *J. Am. Soc. Mass Spectrom.*, 2013, **24**, 932–940.
39 D. G. Harman and S. J. Blanksby, Investigation of the Gas Phase Reactivity of the 1-Adamantyl Radical Using a Distonic Radical Anion Approach, *Org. Biomol. Chem.*, 2007, **5**, 3495–3503.
40 S. Gronert, Estimation of Effective Ion Temperatures in a Quadrupole Ion Trap, *J. Am. Soc. Mass Spectrom.*, 1998, **9**, 845–848.
41 W. A. Donald, G. N. Khairallah and R. A. J. O'Hair, The Effective Temperature of Ions Stored in a Linear Quadrupole Ion Trap Mass Spectrometer, *J. Am. Soc. Mass Spectrom.*, 2013, **24**, 811–815.
42 Normalized collision energy is a term used by the instrument vendor as explained here: https://static.thermoscientific.com/images/D13507~.pdf. Zero, on this scale, means that no additional resonant excitation is applied.
43 T. Su and M. T. Bowers, Ion-Polar Molecule Collisions: The Effect of Ion Size on Ion-Polar Molecule Rate Constants; the Parameterization of the Average-Dipole-Orientation Theory, *Int. J. Mass Spectrom. Ion Phys.*, 1973, **12**, 347–356.
44 Y. Zhao and D. G. Truhlar, The M06 Suite of Density Functionals for Main Group Thermochemistry, Thermochemical Kinetics, Noncovalent Interactions, Excited States, and Transition Elements: Two New Functionals and Systematic Testing of Four M06-Class Functionals and 12 Other Functionals, *Theor. Chem. Acc.*, 2008, **120**, 215–241.
45 L. A. Curtiss, P. C. Redfern, K. Raghavachari and J. A. Pople, Gaussian-3X (G3X) Theory: Use of Improved Geometries, Zero-Point Energies, and Hartree–Fock Basis Sets, *J. Chem. Phys.*, 2001, **114**, 108–117.
46 M. J. Frisch, G. W. Trucks, H. B. Schlegel, G. E. Scuseria, M. A. Robb, J. R. Cheeseman, G. Scalmani, V. Barone, B. Mennucci, G. A. Petersson, H. Nakatsuji, M. Caricato, X. Li, H. P. Hratchian, A. F. Izmaylov, J. Bloino, G. Zheng, J. L. Sonnenberg, M. Hada, M. Ehara, K. Toyota, R. Fukuda, J. Hasegawa, M. Ishida, T. Nakajima, Y. Honda, O. Kitao, H. Nakai, T. Vreven, J. A. Montgomery, J. E. Peralta, F. Ogliaro, M. Bearpark, J. J. Heyd, E. Brothers, K. N. Kudin, V. N. Staroverov, R. Kobayashi, J. Normand, K. Raghavachari, A. Rendell, J. C. Burant, S. S. Iyengar, J. Tomasi, M. Cossi, N. Rega, J. M. Millam, M. Klene, J. E. Knox, J. B. Cross, V. Bakken, C. Adamo, J. Jaramillo, R. Gomperts, R. E. Stratmann, O. Yazyev, A. J. Austin, R. Cammi, C. Pomelli, J. W. Ochterski, R. L. Martin, K. Morokuma, V. G. Zakrzewski, G. A. Voth, P. Salvador, J. J. Dannenberg, S. Dapprich, A. D. Daniels, Ö. Farkas, J. B. Foresman, J. V. Ortiz, J. Cioslowski and D. J. Fox, *Gaussian 09, Revision A.02*, 2009.
47 J. Zheng, Y. Zhao and D. G. Truhlar, The DBH24/08 Database and Its Use to Assess Electronic Structure Model Chemistries for Chemical Reaction Barrier Heights, *J. Chem. Theory Comput.*, 2009, **5**, 808–821.
48 E. Dorrestijn, R. Pugin, M. V. Ciriano Nogales and P. Mulder, Thermal Decomposition of Chroman. Reactivity of o-Quinone Methide, *J. Org. Chem.*, 1997, **62**, 4804–4810.
49 G. da Silva and J. W. Bozzelli, Quantum Chemical Study of the Thermal Decomposition of o-Quinone Methide (6-Methylene-2,4-Cyclohexadien-1-One), *J. Phys. Chem. A*, 2007, **111**, 7987–7994.
50 K. K. Thoen, J. Pérez, J. J. Ferra and H. I. Kenttämaa, Synthesis of Charged Phenyl Radicals and Biradicals by Laser Photolysis in a Fourier-Transform Ion Cyclotron Resonance Mass Spectrometer, *J. Am. Soc. Mass Spectrom.*, 1998, **9**, 1135–1140.
51 J. L. Heidbrink, K. K. Thoen and H. I. Kenttämaa, Polar Effects on Iodine Atom Abstraction by Charged Phenyl Radicals, *J. Org. Chem.*, 2000, **65**, 645–651.
52 L. Jing, J. J. Nash and H. I. Kenttämaa, Correlation of Hydrogen-Atom Abstraction Reaction Efficiencies for Aryl Radicals with Their Vertical Electron Affinities and the Vertical Ionization Energies of the Hydrogen-Atom Donors, *J. Am. Chem. Soc.*, 2008, **130**, 17697–17709.
53 Y. Murakami, T. Oguchi, K. Hashimoto and Y. Nosaka, Theoretical Study of the Benzyl + O_2 Reaction: Kinetics, Mechanism, and Product Branching Ratios, *J. Phys. Chem. A*, 2007, **111**, 13200–13208.
54 D. H. Ess, S. E. Wheeler, R. G. Iafe, L. Xu, N. Çelebi-Ölçüm and K. N. Houk, Bifurcations on Potential Energy Surfaces of Organic Reactions, *Angew. Chem., Int. Ed.*, 2008, **47**, 7592–7601.

